

Supporting Information

Ultra-high-throughput Production of Monodisperse and Multifunctional Janus Microparticles using in-air Microfluidics

Tom Kamperman, Vasileios Trikalitis, Marcel Karperien, Claas Willem Visser, and Jeroen Leijten**

Dr. T. Kamperman, V.D. Trikalitis M.Sc., Prof. M. Karperien, Dr. J. Leijten

Department of Developmental BioEngineering, MIRA Institute for Biomedical Technology and Technical Medicine, University of Twente, Drienerlolaan 5, 7522 NB Enschede, The Netherlands.

Dr. C.W. Visser

Wyss Institute for Biologically Inspired Engineering and John A. Paulson School of Engineering and Applied Sciences, Harvard University, Cambridge, MA 02138, USA
Physics of Fluids Group, Faculty of Science and Technology, University of Twente, Drienerlolaan 5, 7522 NB Enschede, The Netherlands

* Email: t.kamperman@utwente.nl, j.c.h.leijten@utwente.nl

Contents

Experimental Section; Figure S1; Figure S2; Figure S3; Figure S4; Figure S5; Table S1

Experimental Section

IAMF setup operation: The IAMF setup (IamFluidics BV) was equipped with tapered nozzles (31-33 gauge) that were connected to plastic syringes (5 or 10 ml with Luer-Lok) using fluorinated ethylene propylene tubing (FEP, inner diameter 500 μm) and Polyetheretherketone connectors. Low-pressure syringe pumps (neMESYS, Cetoni) were used to control the flow rate. The IAMF setup's piezoelectric nozzle actuator was operated using a 20 Vpp square wave with a frequency between 1 and 15 khz, which was fine-tuned at the beginning of every experiment to obtain optimal microjet breakup. The microjets were aligned using the IAMF setup's micrometer-precision multi-axes adjusters, and microjet coalescence and breakup were confirmed by visual inspection via the setup's high-speed microscope camera (**Movie S1**).

Jet coalescence visualization: The high-speed microscopic images of coalescing and encapsulating drops and microjets were recorded using a previously described stroboscopic visualization setup.¹ In short, an Nd:YAG laser with a pulse duration of 6 ns was directed onto a fluorescent diffuser to generate a homogenous background illumination. A camera (PCO Sensicam QE) with a shutter time of 400 ns was synchronized with these flashes to capture high-resolution snapshots of the experiments. For fluorescent imaging (Figure 1d), rhodamine B (Sigma Aldrich) was added to one of the two microjets.

Janus microparticle production and analysis: Janus microparticles were produced by ejecting and coalescing two microjets that contained 0.5% (w/v) sodium alginate (80 to 120 cP, Wako Chemicals) in H₂O, and a third microjet that contained 0.2M calcium chloride (CaCl₂, Sigma Aldrich) and 10% (v/v) ethanol in H₂O. The liquids were typically ejected at 0.7, 1.8, and 7.2 ml/min using 50, 100, and 250 μm nozzles, respectively. The ejected liquids were thus characterized by $We \sim 25$. Using typical collisional angles of $\sim 40^\circ$, this corresponded to $We_{\text{impact}} \sim 10$. If necessary, microjets were slightly misaligned to achieve

drop-jet and jet-jet coalescence and prevent ‘stretching separation’ effects that may result from head-on collisions.² For fluorescent visualization and analysis, 0.1% (w/v) red or green fluorescent nanoparticles (polystyrene 600 nm, Thermo Fisher Scientific) was added to the alginate containing precursor solution. The microgels were collected in 0.2M CaCl₂ containing H₂O. Microgels and microfibers were visualized using fluorescence microscopy (EVOS FL) and size distributions were determined using the ‘imfindcircles’ function in Matlab. Cross-sectional fluorescent intensity plots were obtained using ImageJ. To produce paramagnetic Janus microparticles, 0.25% (w/v) amino superparamagnetic microparticles (1-2 μm, Polysciences GmbH) were added to the alginate containing precursor solution. To produce multi-enzymatic microreactors, 10 U/ml horseradish peroxidase (HRP, type VI, Sigma Aldrich) and 250 U/ml glucose oxidase (GOX, from *Aspergillus niger*, Type VII, Sigma Aldrich) were added to the alginate containing precursor solution.

Magnetic steering of microparticles: Paramagnetic Janus microparticles were manually steered using a neodymium magnet (5 x 25 mm cylinder, grade N48) from a distance of ~1mm, which resulted in a magnetic field $B \sim 0.25$ T. Particle trapping and steering experiments under continuous flow conditions were performed in a fluidic co-flow chip, which was composed of a channel (500 μm wide, 250 μm high) that was connected to three inlets (**Movie S2**).

Microfluidic co-flow chip: Particle trapping and steering experiments under continuous flow conditions were performed in a microfluidic co-flow chip, which was composed of a channel (500 μm wide, 250 μm high) that was connected to three inlets. The chip was fabricated from polydimethylsiloxane (Sylgard 184, Dow Corning) and glass microscopy slides using standard soft lithography techniques and connected to plastic syringes (5 ml with Luer-Lok) using FEP tubing. Three low-pressure syringe pumps were operated at a flow rate of 10 μl/min to generate a laminar triple co-flow (Reynolds number $Re \sim 1$, $V \sim 4$ mm/s).

Diluted red and yellow ink were used to visualize the triple co-flow. The paramagnetic Janus microparticles were steered by manually positioning the magnet atop the co-flow device. On-chip microphotographs and videos were recorded using a stereomicroscope set-up (Nikon SMZ800 equipped with Leica DFC300 FX camera).

Multi-enzymatic cascade reaction: Paramagnetic HRP/GOX-laden Janus microparticles were trapped within the microfluidic co-flow chip. The triple co-flow was generated by injecting 100 mM β -D-glucose (Sigma Aldrich) in H₂O, H₂O, and 1x 3,3'-diaminobenzidine (DAB) tetrahydrochloride substrate (Thermo Fisher Scientific) in H₂O. Using manual positioning, the paramagnetic GOX/HRP Janus particles were successively exposed for 15 minutes to β -D-glucose, washed in H₂O for a few seconds, and reacted with DAB for 15 minutes. To determine the multi-enzyme dependency of the reaction, the microparticles were incubated in β -D-glucose only, DAB only, and the combination of β -D-glucose and DAB, and subsequently visualized using brightfield microscopy. Poly(DAB) formation was quantified by measuring the absorption in the blue color channel using ImageJ software. To analyze statistical significance, AVOVA with Tukey's post hoc tests was performed using OriginPro software.

Literature study: The gray circles in Figure 2e were obtained from studies based on a Pubmed search (December 2017) including the search entries 'droplet microfluidics janus', 'janus microparticle microfluidic fabrication', and 'janus microparticle microfluidics'.

Schematics: Schematics were made using OriginPro, ChemDraw Professional, and Coreldraw software.

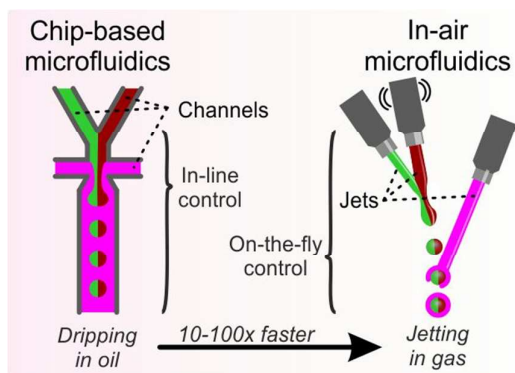


Figure S1. Comparing chip-based microfluidics to in-air microfluidics (IAMF). IAMF is a chip-free platform technology where the channels of conventional microfluidic chips are replaced by micrometer-sized liquid microjets that are combined and controlled in mid-air. This approach enables on-the-fly generation and manipulation (e.g., solidification) of monodisperse Janus microdroplets at jet speed, which is intrinsically 10-100x faster as compared to on-chip dripping.

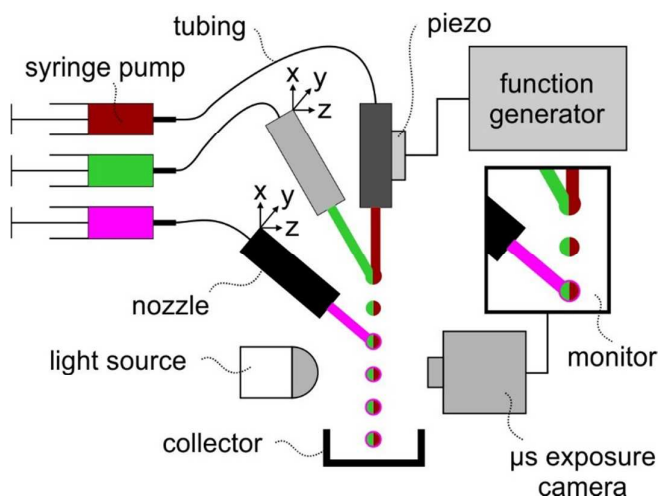


Figure S2. Schematic of the IAMF setup. Liquids are ejected from nozzles that are mounted on multi-axes translation stages. One of the nozzles is piezo-electrically actuated using a function generator. The liquid microjets are visualized using a LED light source and a camera set at exposure time $< 10 \mu\text{s}$ and equipped with a 10-100x zoom lens.

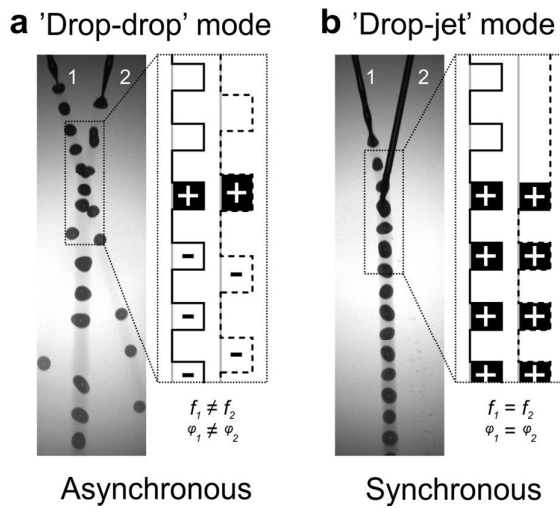


Figure S3. Liquid microjet synchronization in ‘drop-drop’ and ‘drop-jet’ collisional modes. (a) Example of ‘drop-drop’ mode with asynchronous droplet trains. It is often not trivial to synchronize the frequency f and phase φ of two droplet trains, for example, because the droplet depends on the liquid viscosity, nozzle actuation frequency, and microjet speed.³ (b) In contrast, the ‘drop-jet’ mode omits the challenge of synchronizing multiple droplet trains, and effectively results in 100% coalescence.

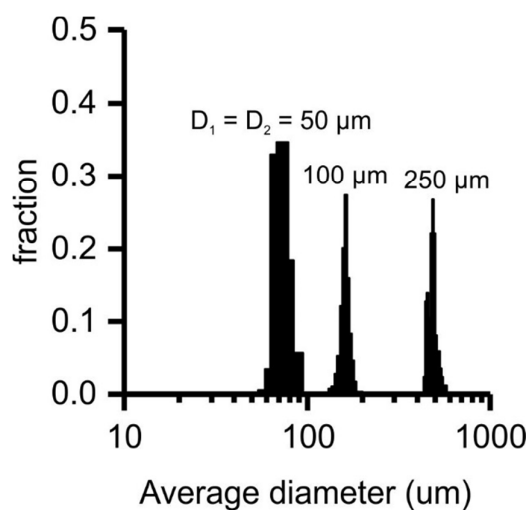


Figure S4. Janus microparticles' size distributions. The Janus microparticle diameter was controlled by tuning the Janus precursor microjet diameter using different nozzle diameters ($D_{1,2}$).

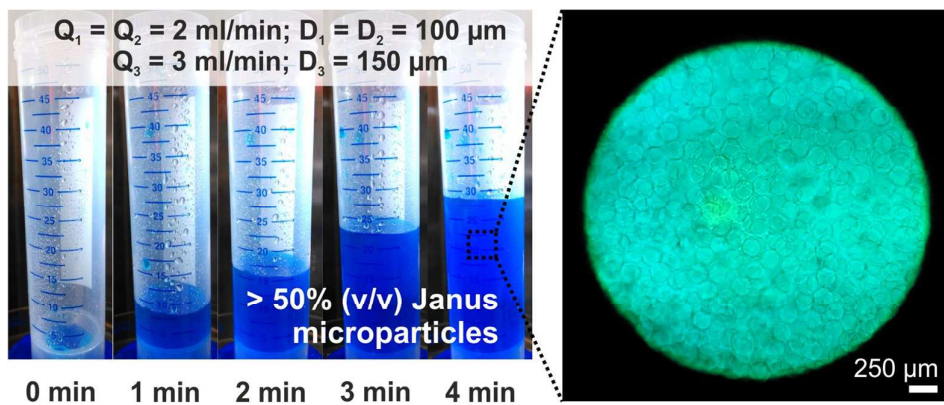


Figure S5. Result of a typical Janus microparticle production process. The Janus precursor microjet was formed by coalescing two alginate containing precursor liquids that were ejected with a flow rate $Q_{1,2} = 2$ ml/min from nozzles with equal diameters $D_{1,2} = 100$ μm . The resulting Janus precursor droplets were on-the-fly combined with a Ca^{2+} containing crosslinker microjet that was ejected with a flow rate $Q_3 = 3$ ml/min from a nozzle with diameter $D_3 = 150$ μm . This effectively resulted in >25 ml of >50% (v/v) Janus microparticles being produced within 4 minutes. Blue ink was added to the Janus microjet for visualization purposes.

Table S1. Data points in Figure 2e, as obtained from studies based on a Pubmed search (December 2017) including the search entries ‘droplet microfluidics janus’, ‘janus microparticle microfluidic fabrication’, and ‘janus microparticle microfluidics’.

Reference	Particle diameter (m)	Flow rate (ml/min)
4	5.90E-05	6.67E-05
4	4.00E-05	6.67E-05
5	1.40E-04	4.00E-03
6	1.85E-04	5.00E-02
7	1.50E-04	2.50E-03
7	3.00E-04	2.50E-03
8	1.00E-04	1.67E-02
9	9.20E-05	2.0E-03
10	1.423E-4	2.13

References

- (1) Visser, C. W.; Frommhold, P. E.; Wildeman, S.; Mettin, R.; Lohse, D.; Sun, C. Dynamics of high-speed micro-drop impact: numerical simulations and experiments at frame-to-frame times below 100 ns. *Soft matter* **2015**, *11* (9), 1708-1722, DOI: 10.1039/c4sm02474e.
- (2) Chen, C., Lin. Collisions of a string of water drops on a water jet of equal diameter. *Experimental Therman and Fluid Science* **2006**, *31*, 6, DOI: 10.1016/j.expthermflusci.2005.11.003.
- (3) Suverkrup, R.; Eggerstedt, S. N.; Gruner, K.; Kuschel, M.; Sommerfeld, M.; Lamprecht, A. Collisions in fast droplet streams for the production of spherolyophilisates. *European journal of pharmaceutical sciences : official journal of the European Federation for Pharmaceutical Sciences* **2013**, *49* (4), 535-541, DOI: 10.1016/j.ejps.2013.05.010.
- (4) Lan, J.; Chen, J.; Li, N.; Ji, X.; Yu, M.; He, Z. Microfluidic generation of magnetic-fluorescent Janus microparticles for biomolecular detection. *Talanta* **2016**, *151*, 126-131, DOI: 10.1016/j.talanta.2016.01.024.
- (5) Seiffert, S.; Romanowsky, M. B.; Weitz, D. A. Janus microgels produced from functional precursor polymers. *Langmuir* **2010**, *26* (18), 14842-14847, DOI: 10.1021/la101868w.
- (6) Chen, Y.; Nurumbetov, G.; Chen, R.; Ballard, N.; Bon, S. A. Multicompartmental Janus microbeads from branched polymers by single-emulsion droplet microfluidics. *Langmuir* **2013**, *29* (41), 12657-12662, DOI: 10.1021/la402417h.
- (7) Hu, Y.; Wang, S.; Abbaspourrad, A.; Ardekani, A. M. Fabrication of shape controllable Janus alginate/pNIPAAm microgels via microfluidics technique and off-chip ionic cross-linking. *Langmuir* **2015**, *31* (6), 1885-1891, DOI: 10.1021/la504422j.
- (8) Lone, S.; Kim, S. H.; Nam, S. W.; Park, S.; Cheong, I. W. Microfluidic preparation of dual stimuli-responsive microparticles and light-directed clustering. *Langmuir* **2010**, *26* (23), 17975-17980, DOI: 10.1021/la103367v.
- (9) Marquis, M.; Davy, J.; Cathala, B.; Fang, A.; Renard, D. Microfluidics assisted generation of innovative polysaccharide hydrogel microparticles. *Carbohydr Polym* **2015**, *116*, 189-199, DOI: 10.1016/j.carbpol.2014.01.083.
- (10) Nisisako, T.; Ando, T.; Hatsuzawa, T. High-volume production of single and compound emulsions in a microfluidic parallelization arrangement coupled with coaxial annular world-to-chip interfaces. *Lab Chip* **2012**, *12* (18), 3426-3435, DOI: 10.1039/c2lc40245a.